Laser performance of a broadband wavelength tunable Yb:germanophosphate glass with direct diode pumping

Hai Yu (余 海)[1,4], Yaqiao Liu (刘亚樵)[1], Jie Guo (郭 洁)[1,4], Liyan Zhang (张丽艳)[2],
Hua Lin (林 华)[1], and Xiaoyan Liang (梁晓燕)[1,3,*]

[1]*State Key Laboratory of High Field Laser Physics, Shanghai Institute of Optics and Fine Mechanics, Chinese Academy of Sciences, Shanghai 201800, China*
[2]*Key Laboratory of Materials for High Power Laser, Shanghai Institute of Optics and Fine Mechanics, Chinese Academy of Sciences, Shanghai 201800, China*
[3]*School of Physical Science and Technology, Shanghai Tech University, Shanghai 200031, China*
[4]*University of Chinese Academy of Sciences, Beijing 100049, China*
**Corresponding author: liangxy@siom.ac.cn*

Received December 26, 2016; accepted April 7, 2017; posted online April 28, 2017

The laser performance of a new Yb:germanophosphate (Yb:GP) glass is investigated. A maximum output power of 826 mW at 1063 nm is achieved with direct diode pumping at 976 nm. The wavelength is tuned from 1034.47 to 1070.83 nm, corresponding to a tuning range of 36.36 nm. Thermal lens effects are investigated to optimize the optical cavity.

OCIS codes: 140.3580, 140.3615, 140.3600, 140.6810.
doi: 10.3788/COL201715.071406.

Solid-state lasers have been widely applied in many fields, including nonlinear frequency conversion, nonlinear microscopy, surface physics, and precision manufacturing because of high efficiency, large tunable range and good beam quality[1–6]. In general, the output power and efficiency of a laser system are mainly determined by properties of gain mediums. Glass gain mediums possess low manufacturing costs, attainable large apertures, and smooth fluorescence spectra. These properties make glass gain mediums competent potential applicants for tunable laser sources and ultra-short pulse generation[7,8].

Among various diode-pumped all-solid-state laser glass gain mediums, Yb^{3+}-doped glass has gained significant attention due to their excellent characteristics such as large absorption coefficient, long energy-storage lifetime, and small quantum defect, leading to less heat generation, high slope efficiency, and good beam quality[7]. In recent years, several glass materials doped with Yb^{3+} ions have made great progress due to their capability of being pumped by high-power diode lasers in the 900–1000 nm region[9–12]. 2.8 W CW output power was achieved by Liu *et al.* with a special water-cooled device on thin Kigre QX phosphate glass, which corresponds to a slope of 15%[13]. Jaque *et al.* used a 2 mm thick Yb phosphate glass to demonstrate a laser slope as high as 53% and an output power of 0.8 W for a diode-pumped Yb^{3+} laser operating at room temperature[14]. A broadband wavelength-tunable glass laser was obtained by Loeser *et al.* maintaining a tunable range of 80 nm and output power of 250 mW based on $Yb:SiO_2$ multicomponent glass[15]. Röser *et al.* enlarged the tuning range by using Yb-doped fused silica glass rods, producing a 100 nm tunable range with 350 mW maximum output power[16].

Although several materials based on Yb glass have been successful demonstrated, two main disadvantages: low emission cross section and serious thermal load of gain media, limit the laser performance significantly[17,18]. Several solutions have been adopted to overcome these problems. One solution is adding novel compounds into host materials to change cross sections and lifetime[19]. Different concentrations of host materials and doping iron can affect the glass performance[20,21]. Additionally, thermal effects can be decreased by being water cooled and producing a thin glass configuration[13,14].

In this Letter, a new type of Yb:germanophosphate (Yb:GP) glass $[(75P_2O_5\text{-}3Al_2O_3\text{-}4K_2O\text{-}10BaO\text{-}3Nb_2O_3\text{-}5B_2O_3)\text{-}3Yb_2O_3\text{-}20GeO_2]$ was investigated, and the emission cross section was increased by doping GeO_2. To promote the optical resonator design and match the mode on the gain medium, the thermal lens effect was measured and compensated. The maximum output power (826 mW) at 1063 nm with a slope efficiency of 9.41% and an optical-to-optical conversion efficiency up to 8% was achieved using an absorbed pump power of 8.772 W at 976 nm. The tuning range was from 1034.47 to 1070.83 nm, with the curve peak achieved at approximately 1056.42 nm, and a tunable range of 36.36 nm. To the best of our knowledge, this is the first time a laser base on Yb:GP glass was produced.

Figure 1 shows the room-temperature fluorescence intensity of conventional Yb:phosphate glass and Yb:GP glass, respectively. Yb:GP glass has a wide bandwidth, and a higher intensity near 1060 nm, making it a better applicant for gain mediums. Figure 2 shows the experimental structure of the Yb:GP glass laser.

The pump source was a fiber-coupled diode laser with a core diameter of 200 μm and numerical aperture (NA) of

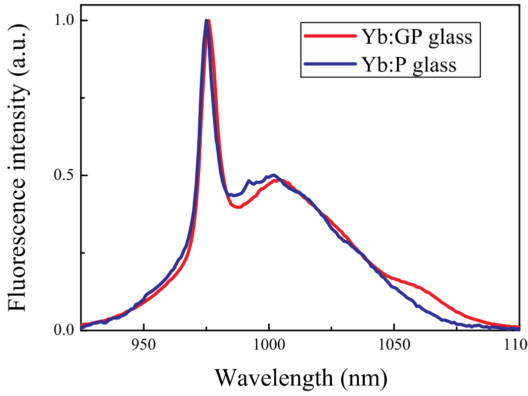

Fig. 1. Room-temperature fluorescence intensity of Yb:GP and Yb:phosphate (Yb:P) glass.

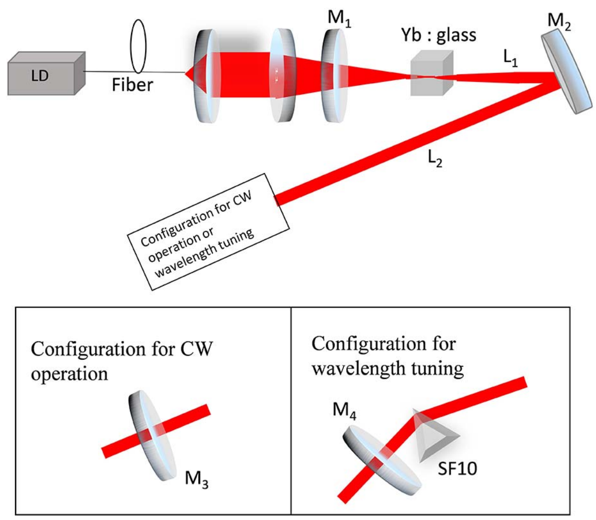

Fig. 2. Schematic of the experimental setup.

0.22, emitting at a central wavelength of 976 nm; a series of 9.45 at. % doped Yb:GP glasses with the sizes of 3 × 3 × 3 (mm) and 3 × 3 × 4 (mm), respectively, were used as gain mediums, which were all wrapped with indium foil and mounted on a water-cooled copper block at a temperature of 15°C. The pump was focused on the glass by using a couple of lenses with an image ratio of 2:1. The laser was composed of a dichroic mirror M_1, a highly reflective concave mirror M_2 with radius of curvature at 300 mm, and a plane output mirror M_3.

In order to optimize the beam quality and improve the optical efficiency, the thermal lens effect was characterized. The thermal lens effect of glass is obvious and dominant at high pump power; the stability zone of the optical cavity is altered and the mode size is decreased[22]. High modes, relatively low optical efficiency, and inferior beam quality were induced by the thermal lens effect[23]. To analyze and adapt the thermal lens effect, the focal length of glass for various pumping powers were calculated through measuring the beam size of the laser output. We obtained a series of beam radii at different places behind M_3 by using a charge-coupled device (CCD) camera. Afterward, the beam radius on M_3 was achieved by fitting the Gaussian beam propagation equation. The Gaussian beam propagation equation is

$$\omega^2(z) = \omega_0^2\left[1 + \left(\frac{M^2\lambda z}{\pi\omega_0^2}\right)^2\right] \tag{1}$$

where ω_0 referrs to the waist spot size, $\omega(z)$ denotes the beam spot size (at the z position considered), and M^2 represents the M^2 factor. The focal lengths of the thermal lens were simulated from the Gaussian beam transformation in the optical resonator. The beam radius on the glass were achieved at the same time. Figure 3 shows the thermal focal lengths and the beam radii on the glass versus absorbed pump power.

Several standards were considered to promote the optical resonator to match the thermal effects and accommodate the stability region[24]. The variation of the mode size produced by the thermal lens effect should be as small as possible. The stability zone of the solid-state laser resonator should be insensitive to this effect. Given the focal lengths of thermal lens of the glass, L_1 and L_2 were optimized to 140 and 168 mm, respectively.

Various M_3 transmissions (1%, 4%, and 6%) were used to improve the laser output power and slope efficiency. The highest output efficiency was attained with 4% M_3, and the maximum output power was 826 mW under 6% output transmission (shown in Fig. 4). Compared with 3 × 3 × 4 (mm) glass, 3 × 3 × 3 (mm) glass maintained a high slope efficiency.

The M^2 factor and the beam profile of the laser under 326 mW output power were measured. The output beam was obtained with a CCD camera. The results delivered a beam quality of $M_x^2 = 1.01$, $M_y^2 = 1.01$ in both directions perpendicular to the axis of the propagation (shown in Fig. 5), which is close to the diffraction limit, revealing an excellent TEM_{00} mode.

An SF10 dispersive prism was introduced into the output arm of the laser cavity to obtain a wave. The output

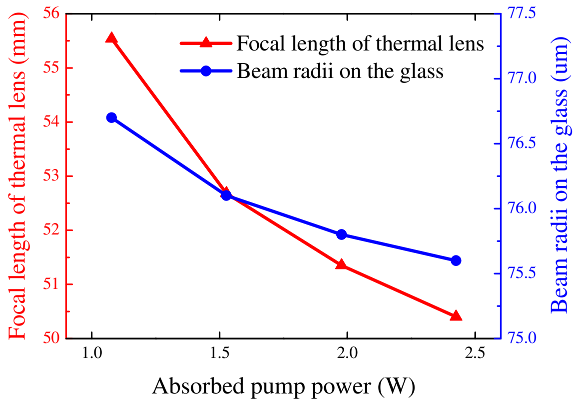

Fig. 3. Focal length of the thermal lens and beam radii on the glass versus the absorbed pump power for the Yb:GP glass sample.

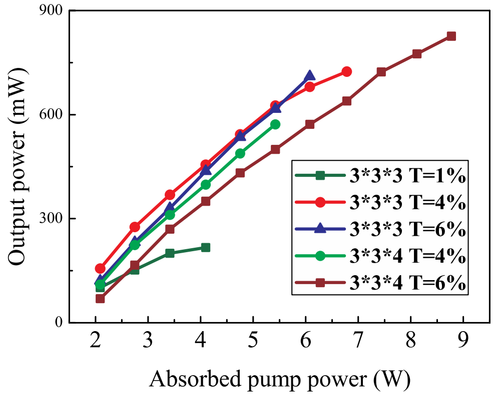

Fig. 4. Output power versus the absorbed pump power for the Yb:GP glass.

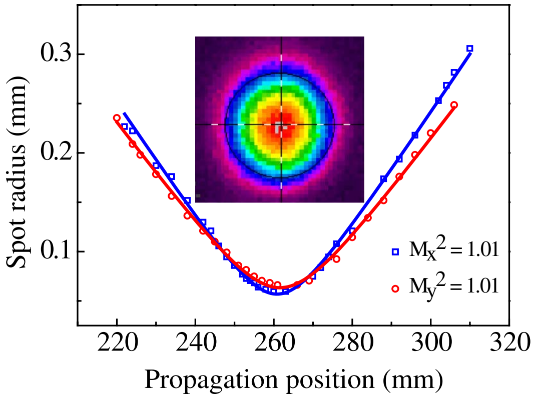

Fig. 5. Beam quality and M^2 factor for both directions perpendicular to the axis of propagation.

mirror with $T = 1\%$ was applied during wavelength tuning. The wavelength was tuned from 1034.47 to 1070.83 nm, corresponding to a tuning range of 36.36 nm, as shown in Fig. 6. The peak emission occurred at 1056.42 nm. Further tuning on a shorter wavelength was limited by the coating of the dichroic mirror.

In conclusion, we investigate the laser performance of Yb:GP glass. The thermal lens effect is considered to compensate and design the cavity. The focal length of the sample and beam radii on the glass are obtained. The maximum output power of 826 mW at 1063 nm is achieved. The broadband wavelength ranges from 1034.47 to 1070.83 nm, which corresponds to a wide tunable range of 36.36 nm. This is to the best of our knowledge the first time laser output power and a wavelength tunable range using Yb:GP glass is obtained. Experimental results indicate that Yb:GP glass is an excellent source for tunable laser and ultra-short pulse generation.

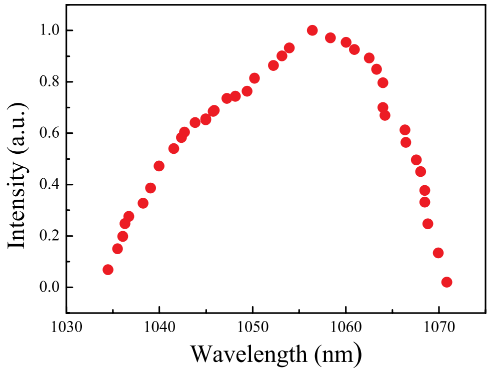

Fig. 6. Wavelength tuning in the CW regime.

This work was supported by the National Science Foundation of China (NSFC) under Grant Nos. 11504394, 61521093, and 61378030.

References

1. G. Huber, C. Kränkel, and K. Petermann, J. Opt. Soc. Am. **27**, B93 (2010).
2. Y. Kalisky and O. Kalisky, Opt. Eng. **49**, 091003 (2010).
3. P. Zhu, D. Li, Q. Liu, J. Chen, S. Fu, P. Shi, K. Du, and P. Loosen, Opt. Lett. **38**, 4716 (2013).
4. R. J. Gray, X. H. Yuan, D. C. Carroll, C. M. Brenner, M. Coury, M. N. Quinn, O. Tresca, B. Zielbauer, B. Aurand, V. Bagnoud, J. Fils, T. Kuhl, X. Lin, C. Li, Y. Li, M. Roth, D. Neely, and P. McKenna, Appl. Phys. Lett. **99**, 171502 (2011).
5. J. Kleinbauer, R. Knappe, and R. Wallenstein, Appl. Phys. B **80**, 315 (2005).
6. X. Fu, J. Li, and X. Liang, Chin. Opt. Lett. **11**, 051402 (2013).
7. C. Hönninger, F. Morier-Genoud, M. Moser, and U. Keller, Opt. Lett. **23**, 126 (1998).
8. W. F. Krupke, IEEE J. Quantum Electron. **6**, 1287 (2000).
9. R. Koch, W. A. Clarkson, D. C. Hanna, S. Jiang, M. J. Myers, D. Rhonehouse, S. J. Hamlin, U. Griebner, and H. Schonnagel, Opt. Commum. **134**, 175 (1997).
10. S. Ohara and Y. Kuroiwa, Opt. Express **17**, 14104 (2009).
11. Z. Liu, C. Qi, S. Dai, Y. Jiang, and L. Hu, Chin. Opt. Lett. **1**, 37 (2003).
12. J. Liu, J. Tian, Z. Dou, M. Hu, and Y. Song, Chin. Opt. Lett. **13**, 061407 (2015).
13. H. Liu, J. Paye, S. Biswal, J. Nees, X. Liu, and G. Mourou, in *Proceedings of Conference on Lasers and Electro-Optics* (1998), p. 177.
14. D. Jaquea, J. C. Lagomacini, C. Jacinto, and T. Catunda, Appl. Phys. Lett. **89**, 121101 (2006).
15. M. Loeser, F. Röser, A. Reichelt, M. Siebold, S. Grimm, D. Litzkendorf, A. Schwuchow, J. Kirchhof, and U. Schramm, Opt. Lett. **37**, 4029 (2012).
16. F. Röser, M. Loeser, D. Albach, M. Siebold, S. Grimm, D. Brand, A. Schwuchow, A. Langner, G. Schotz, D. Schonfeld, and U. Schramm, Opt. Mater. Express **5**, 704 (2015).
17. B. Yang, X. Liu, X. Wang, J. Zhang, L. Hu, and L. Zhang, Opt. Lett. **39**, 1772 (2014).
18. G. Boulon, J. Alloy. Comput. **451**, 1 (2008).
19. L. Zhang, Y. Leng, J. Zhang, and L. Hu, J. Mater. Sci. Technol. **26**, 921 (2010).
20. J. Šulc, R. Švejkar, H. Jelínková, K. Nejezchleb, K. Nitsch, A. Cihlář, R. Král, M. Ledinský, A. Fejfar, M. Rodová, P. Zemenová, and M. Nikl, Opt. Eng. **55**, 047102 (2016).
21. L. Zhang, T. Xue, D. He, M. Guzik, and G. Boulon, Opt. Express **23**, 1505 (2015).
22. J. Steffen, J. P. Lortsche, and G. Herziger, IEEE J. Quantum Electron. **8**, 239 (1972).
23. L. M. Osterink and J. D. Foster, Appl. Phys. Lett. **12**, 128 (1968).
24. V. Magni, Appl. Opt. **25**, 107 (1986).